Cite this: *Nanoscale*, 2011, **3**, 4434

www.rsc.org/nanoscale

PAPER

Synthesis of micro-nano hierarchical structured $LiFePO_4$/C composite with both superior high-rate performance and high tap density

Meng Wang,[a] Yong Yang[b] and Youxiang Zhang*[a]

Received 27th July 2011, Accepted 24th August 2011
DOI: 10.1039/c1nr10950b

Efforts were made to synthesize $LiFePO_4$/C composites showing both high rate capability and high tap density. First, monoclinic phase $FePO_4 \cdot 2H_2O$ with micro-nano hierarchical structures are synthesized using a hydrothermal method, which are then lithiated to $LiFePO_4$/C also with hierarchical structures by a simple rheological phase method. The primary structures of $FePO_4 \cdot 2H_2O$ are nanoplates with ~30 nm thickness, and the secondary structures of the materials are intertwisted micro-scale rings. The $LiFePO_4$/C materials lithiated from these specially structured precursors also have hierarchical structures, showing discharge capacities of more than 120, 110, and 90 mAh g^{-1} at rates of 5 C, 10 C and 20 C, respectively, and high tap density of 1.4 g cm^{-3} as cathode materials for lithium ion batteries. Since tap density is an important factor that needs to be considered in fabricating real batteries in industry, these hierarchical structured $LiFePO_4$/C moves closer to real and large-scale applications.

1. Introduction

Rechargeable lithium-ion batteries are now considered as the next generation of power sources for applications in electric vehicles (EVs), hybrid electric vehicles (HEVs), and plug-in hybrid electric vehicles.[1–3] The olivine $LiFePO_4$ is an attractive electrode material for these rechargeable lithium-ion batteries due to its low cost, long cycle life, environmental friendliness and thermal stability.[4] However, along with these exceptional advantages, $LiFePO_4$ has long suffered from poor high-rate capacity due to the low electronic conductivity and slow diffusion of lithium ions. To overcome the low electronic conductivity of $LiFePO_4$, tremendous efforts have been made through various material processing approaches.[5–11] Among these approaches, doping of metallic elements in the bulk[5] and coating the particles with carbonaceous conductors on the surface[8] have proved to be effective ways to improve the electronic conductivity of $LiFePO_4$ particles. To improve the high-rate performance, the $LiFePO_4$ particles are reduced to the nanometre scale to shorten the diffusion length for electrons and lithium ions and to increase the effective reaction areas.[12–15]

However, in addition to rate capability, energy density is also one of the most important characteristics of electrode materials for practical applications. To increase the high-rate performance solely by reducing the particle size will increase the surface area of the materials, which result in larger mass fractions of carbon needed to coat the particles to the same thickness. Since carbon is inactive and bulky, a large amount of carbon decreases both the volumetric and the gravimetric energy density of the $LiFePO_4$/C composites significantly. Tap density, which is well correlated to the density that can be achieved in coated electrodes, is also sacrificed if the rate capability of the $LiFePO_4$/C composites is increased solely by synthesizing nano-sized particles.[16,17] Furthermore, in the process of manufacturing real batteries, the $LiFePO_4$/C cathode materials need to be spread onto aluminum foil which is used as the current collector. Nano-sized particles will fall off the current collector easily and then tap density of the materials is an important factor that needs to be considered. Generally the $LiFePO_4$/C composites with simple nanoscale particles have very small tap density (less than 1.0 g cm^{-3}), while tap density as high as 1.6 g cm^{-3} can be reached for micro-sized $LiFePO_4$/C composites.[18] Thus, the ideal structures for $LiFePO_4$ should have hierarchical structures, with nanosized primary structures to ensure high rate capability and micro-sized secondary structures to guarantee a high tap density.

In this paper, monoclinic phase $FePO_4 \cdot 2H_2O$ with micro-nano hierarchical structures are synthesized using a hydrothermal method and are lithiated to $LiFePO_4$/C with the same hierarchical structures by a simple rheological phase method. The $LiFePO_4$/C composites lithiated from these specially structured precursors show both excellent high-rate performance and high tap density as the cathode for lithium ion batteries. The tap density is 1.4 g cm^{-3} while the discharge capacities of more than 120, 110 and 90 mAh g^{-1} are achieved at rates of 5 C, 10 C and 20 C, respectively, at room temperature.

[a]*College of Chemistry and Molecular Sciences, Wuhan University, Wuhan, 430072, China. E-mail: yxzhang04@whu.edu.cn; Fax: +86-27-6875-4067; Tel: +86-27-6578-3395*
[b]*State Key Laboratory for Physical Chemistry of Solid Surfaces, Department of Chemistry, College of Chemistry and Chemical Engineering, Xiamen University, Xiamen, 361005, China*

2. Experimental

Material preparation

The $FePO_4 \cdot 2H_2O$ precursor was synthesized by a hydrothermal method. In a typical synthesis procedure, 3.0 mmol hexadecyl trimethyl ammonium bromide (CTAB) was added to 100 mL of deionized water and stirred for 1 h to form a homogeneous and pellucid solution. Then 4.5 mmol $FeCl_3 \cdot 6H_2O$ was added into the solution and stirred until it was completely dissolved. After that, 1.5 mL of H_3PO_4 solution was dropped into the solution gradually and stirred for another hour. Subsequently, the mixture was sealed in a Teflon®-lined stainless steel autoclave, and heated at 170 °C for 2 h. After cooled to room temperature, the white precipitate was separated by centrifugation for 10 min, washed with water and ethanol several times, and then dried at 100 °C for 4 h.

A simple rheological phase method,[19–21] using the $FePO_4 \cdot 2H_2O$ precursor as sources for both the Fe and P in the materials, was employed to synthesize the $LiFePO_4$/carbon composite. Specifically, stoichiometric amounts of $FePO_4 \cdot 2H_2O$, $LiOH \cdot H_2O$ and polyethylene glycol (PEG) (50.0 g PEG/1 mol $FePO_4 \cdot 2H_2O$) were used as the starting materials. First, $FePO_4 \cdot 2H_2O$, $LiOH \cdot H_2O$, PEG and an appropriate amount of water were mixed and ground for several minutes to get a solid-liquid rheological body, which looks like a kind of mushy slurry. Then the rheological body was calcined at 650 °C in a tube furnace for 6 h under argon flow. After cooling to room temperature, the $LiFePO_4$/carbon composite was obtained.

Physical characterization

Powder X-ray diffraction (Bruker D8 ADVANCE, Germany) using Cu Kα radiation was used to determine the crystalline phase of the synthesized material. The particle morphology and microstructures were observed using a scanning electron microscope (SEM, QUANTA 200, Holland) and a high-resolution transmission electron microscope (HRTEM, JEOL, JEM-2010-FEF, Japan). The thermogravimetric (TG, Netzsch STA 449C, Germany) and related analysis were determined in oxygen from room temperature to 700 °C at a heating rate of 10 °C min^{-1}. To measure the tap density, about 4 g of powder was placed in a small glass vial and tapped on the lab bench for 10 min by hand. The measured volume of the tapped powder and its mass was used to calculate the "tap" density.[16]

Electrode preparation and cell testing

The electrochemical characterizations were performed using a CR2016 coin-type cell. For cathode fabrication, the synthesized $LiFePO_4$/carbon composite was mixed with acetylene black and polytetrafluoroethylene (PTFE) binder with a weight ratio of 80 : 15 : 5. After pressing onto a stainless mesh, which served as a current collector, the cathode film was dried at 120 °C for 6 h in an oven. The loading density of the $LiFePO_4$ within the electrode is 5 mg cm^{-2}. The test cell consisted of a cathode and a lithium foil anode separated by a Celguard 2300 microporous film, and 1 M $LiPF_6$ dissolved in ethylene carbonate (EC)/diethyl carbonate (DEC) (1 : 1 volume ratio) as the electrolyte. The assembly of the cells was carried out in a dry Ar-filled glove box. The cells were galvanostatically charged and discharged between 2.0 V and 4.4 V *versus* Li/Li^+ on a battery cycler (LAND, CT2001A, China). All the electrochemical tests were carried out at room temperature.

3. Results and discussion

The XRD pattern and the TG-DTA curves of the as-synthesized iron phosphates are shown in Fig. 1. The XRD pattern (Fig. 1a) matches well with monoclinic $FePO_4 \cdot 2H_2O$ (phosphosiderite [33-0666], space group $P21/n$, with lattice parameters $a = 0.5329$ nm, $b = 0.9798$ nm, and $c = 0.8710$ nm), suggesting a perfect crystallinity of the as-synthesized samples. From the TG curve (Fig. 1b), we can see that 19.03% of the mass, corresponding to two water molecules in one iron phosphate molecule, was lost in one step at around 200 °C. After that, the mass of the iron phosphates did not change up to 800 °C. In the DTA curve (Fig. 1b), there is an endothermic peak at 193.1 °C and an exothermic peak at 711.4 °C. The first peak corresponds to the reaction of the iron phosphate losing the two water molecules (endothermic reaction). The second peak corresponds to the phase change (exothermic reaction) of the iron phosphate.

The structures of the as-synthesized $FePO_4 \cdot 2H_2O$ were identified by SEM and TEM and their images are shown in Fig. 2. From the SEM images (Fig. 2a and 2b), it is clear that the as-

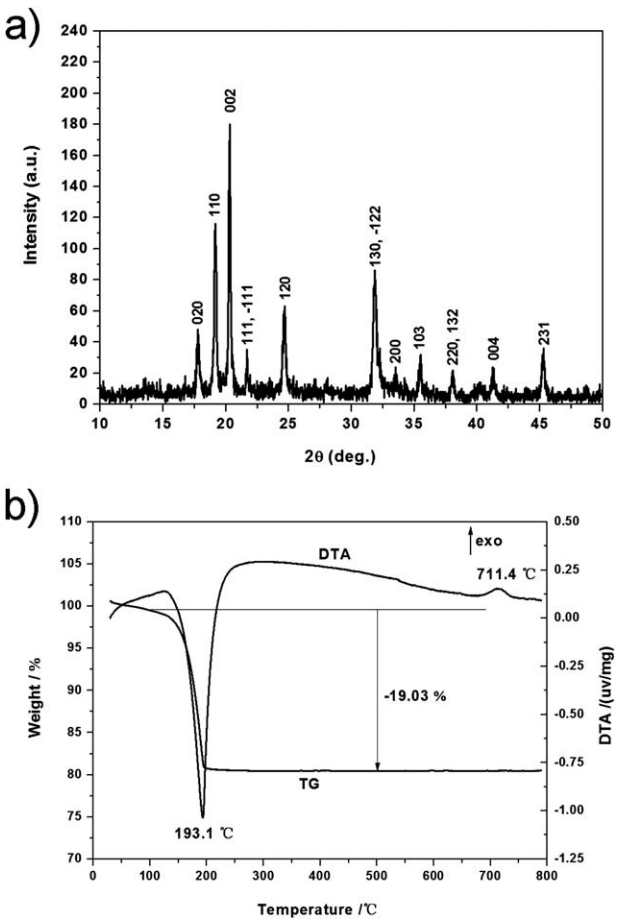

Fig. 1 The XRD pattern and TG-DTA curves of the as-synthesized micro-nano hierarchical structured $FePO_4 \cdot 2H_2O$.

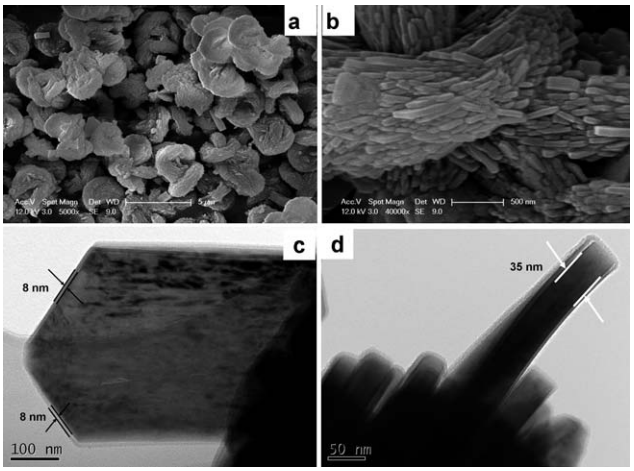

Fig. 2 The SEM (a, b) and TEM (c, d) images of the as-synthesized micro-nano hierarchical structured $FePO_4 \cdot 2H_2O$.

synthesized $FePO_4 \cdot 2H_2O$ have micro-nano hierarchical structures, with nanoplates as the primary structures and intertwisted micro-scale rings as the secondary structures. The TEM images are shown in Fig. 2c and 2d. From these images, we can see that the width of the nanoplates (primary structures) is about 300 nm and their thickness is about 35 nm. There is an amorphous layer, with about 8 nm thickness, on the surface of the nanoplates. This amorphous layer should be a layer of CTAB that was used in the synthesis of $FePO_4 \cdot 2H_2O$ as surfactant. To validate our suspicions we calcinated the as-synthesized $FePO_4 \cdot 2H_2O$ in Ar, and took the XRD of the product. The XRD spectrum is shown as Fig. 3. It was shown that part of the product of the calcination was $Fe_2P_2O_7$ with the Fe^{3+} in $FePO_4 \cdot 2H_2O$ reduced to Fe^{2+} by the CTAB layer on the surface.

As for the formation mechanism, we propose that the adsorbed CTAB surfactant on the particles favored the formation of monoclinic $FePO_4 \cdot 2H_2O$ nanoplates, similar to the formation of monoclinic $BiVO_4$ nanosheets.[22] This kind of crystal formation mode assisted by organic surfactants has been frequently

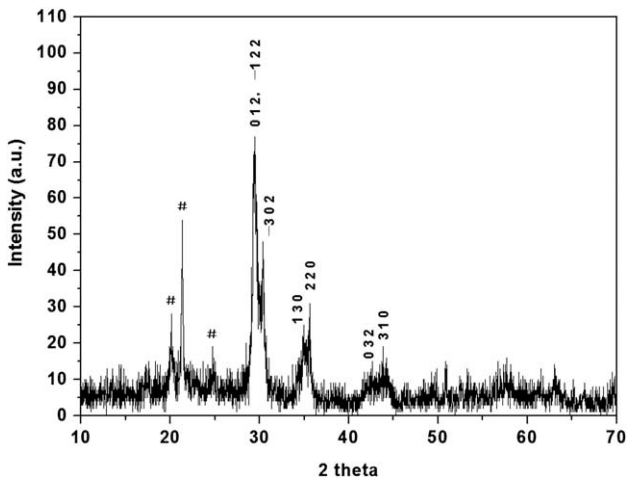

Fig. 3 The XRD pattern of the product after calcinating the as-synthesized $FePO_4 \cdot 2H_2O$ in Ar (the peaks marked with # are from $FePO_4$).

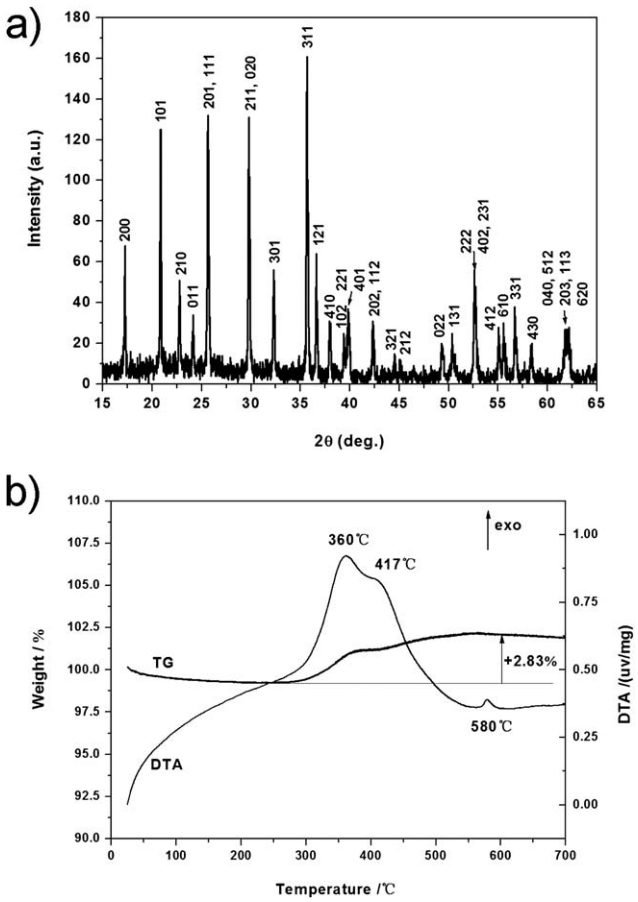

Fig. 4 The XRD pattern and TG-DTA curves of the $LiFePO_4$/C composite synthesized by a rheological phase method using the micro-nano hierarchical structured $FePO_4 \cdot 2H_2O$ as the precursor.

reported recently.[23,24] A very simple way to decrease the thickness of the nanoplates is to decrease the concentrations of the reactants.[20]

The XRD pattern and the TG-DTA curves of the $LiFePO_4$/C composite synthesized using the $FePO_4 \cdot 2H_2O$ micro-nano

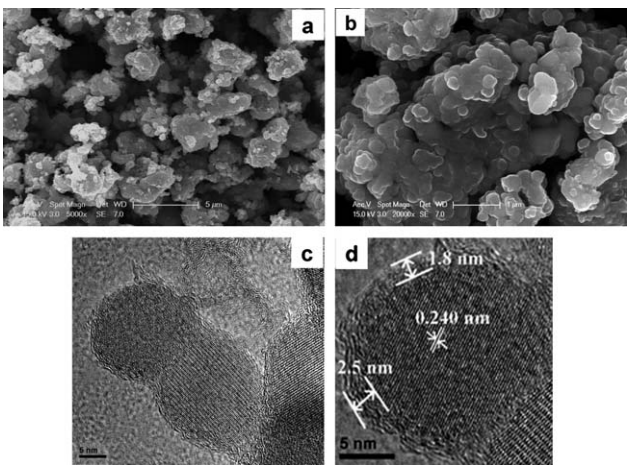

Fig. 5 The SEM (a, b) and TEM (c, d) images of the $LiFePO_4$/C composite.

hierarchical structures as the precursor by a simple rheological phase method are shown in Fig. 4. The entire XRD pattern (Fig. 4a) matches well with standard orthorhombic $LiFePO_4$ (JCPDS No. 83-2092), suggesting a perfect crystallinity of the synthesized samples with no impurities. The TG-DTA measurement (Fig. 4b) was determined in air from room temperature to 700 °C and was used to estimate the carbon content in the as-synthesized $LiFePO_4$/C composite. From the DTA curve, we can see that three exothermic reactions happened from room temperature to 700 °C. The first exothermic reaction occurred at 360 °C and this should correspond to the oxidation of $LiFePO_4$ to $Li_3Fe_2(PO_4)_3$ and Fe_2O_3. The second exothermic reaction occurred at around 417 °C, corresponding to the oxidation of the carbon in the composite to CO_2 gas. The third exothermic reaction happened at around 580 °C, and this should correspond to the phase change of $Li_3Fe_2(PO_4)_3$ or Fe_2O_3 since

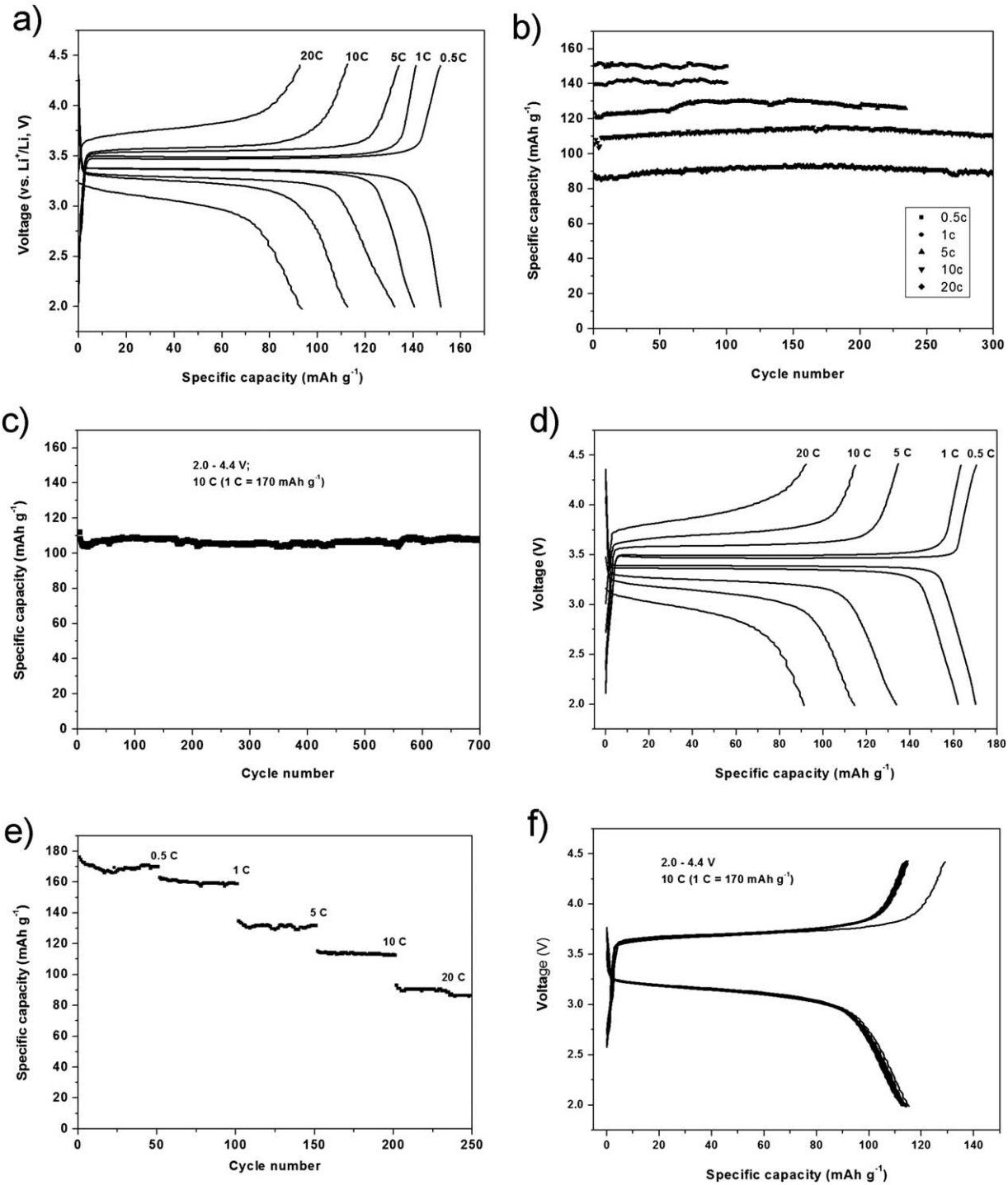

Fig. 6 The electrochemical performances of the hierarchical structured $LiFePO_4$/C composite (a, b, c: with no CNTs; d, e, f: with CNTs).

there is no mass change after 560 °C in the corresponding TG curve. From the TG curve, we can see that the first oxidation reaction ($LiFePO_4$ was oxidized to $Li_3Fe_2(PO_4)_3$ and Fe_2O_3) resulted in weight gain. When the temperature continued to increase, the carbon in the composite started to oxidize to CO_2 gas which resulted in weight loss. The weight gain and the weight loss at the later stage led to the TG curve as shown in Fig. 4b. According to the calculation method proposed by M.S. Whittingham,[25] the amount of carbon in the $LiFePO_4$/C composite should be the theoretical weight gain (5.07%) subtracted by the actual weight gain of the $LiFePO_4$/C composite. Thus the carbon content in the as-synthesized $LiFePO_4$/C composite should be 2.24% (5.07%–2.83%).

The microstructures of the fabricated $LiFePO_4$/C composites were identified by SEM and TEM, and their images are shown in Fig. 5. From the SEM images (Fig. 5a and 5b), we can see that the as-synthesized $LiFePO_4$/C composites keeps the micro-nano hierarchical structures. The primary structures of the composites are nanoscale particles and the secondary structures are micro-scale irregular rings (Fig. 5a). It seems that as the reaction proceeds, the $FePO_4 \cdot 2H_2O$ precursor with nanoplates morphology transforms into $LiFePO_4$/C particles with a quasi-sphere morphology (Fig. 5b). The high-resolution TEM images were shown in Fig. 5c and 5d. As shown in Fig. 5c, $LiFePO_4$/C quasi-spheres with diameters as small as 20 nm can be synthesized by this method. There is a thin layer of amorphous carbon which not only coats the $LiFePO_4$ particles but also interconnects the nanoscale particles together. This layer of carbon nanocoating can increase the electronic conductivity of $LiFePO_4$ particles and is also widely used to improve the performance of metal oxide based anode materials.[26,27] From Fig. 5d, the thickness of the amorphous carbon layer can be measured as about 2 nm.

Fig. 6 shows the electrochemical performances of the hierarchically structured $LiFePO_4$/C composite as the cathode for lithium ion batteries. From Fig. 6a and 6b, it showed that the low rate capability (around 150 and 140 mAh g^{-1} specific capacities at 0.5 C and 1 C, respectively) did not have many advantages over the $LiFePO_4$/C composite with other structures. However, the materials showed excellent high-rate capability. The discharge specific capacities of this micro-nano hierarchically structured $LiFePO_4$/C composite can stabilize at more than 120, 110, and 90 mAh g^{-1} at high rates of 5 C (850 mA g^{-1}), 10 C (1700 mA g^{-1}) and 20 C (3400 mA g^{-1}), respectively. The results shown in Fig. 6c demonstrate that this hierarchically structured $LiFePO_4$/C composite also exhibit an excellent cycling performance. For the 10 C rate performance, almost no obvious capacity loss can be observed for the first 700 cycles. When some carbon nanotubes (CNTs) were mixed into the cathode materials (the weight ratio was 80 : 10 : 5 : 5 for the synthesized $LiFePO_4$/C composite, acetylene black, CNT and polytetrafluoroethylene (PTFE) binder), the low rate capability improved a lot, with the specific capacities reaching 170 and 160 mAh g^{-1} at a rate of 0.5 C and 1 C, respectively (Fig. 6d and 6e). However, the capacities at high rates did not improve much compared to the materials with no CNTs. Fig. 6f showed that the performance at high rates was very stable. Almost no change occurred in the voltage-capacity curves for 50 cycles at a rate of 10 C.

Recently, many $LiFePO_4$/C nanostructures, such as mesoporous $LiFePO_4$/C nanocomposite,[28] carbon coated $LiFePO_4$ nanocrystals,[29] and $LiFePO_4$/C thin nanoplates,[30] were synthesized and all of these $LiFePO_4$/C nanostructures showed excellent high-rate electrochemical performances. The superior performance was believed to be caused by the short transport distances for lithium-ion within the particles and the high specific surface area of the particles which permits a high contact area with the electrolyte and hence a high lithium-ion flux across the interface for these nano-sized thin carbon layer-coated $LiFePO_4$ particles. Consistent with this idea, the $LiFePO_4$/C nanocomposite with smaller sizes[13] thus showed even better performance at higher rates (~90 mAh g^{-1} at about 60 C). But specific capacity at high rates is not the only goal we should pursue. Increasing the high-rate performance just by synthesizing nano-sized particles will decrease both the volumetric and the gravimetric energy density of the $LiFePO_4$/C composites significantly. Also in the process of manufacturing real batteries, the $LiFePO_4$/C cathode materials need to be spread onto aluminum foil (used as the current collector) and then the tap density of the materials is an important factor that needs to be considered. Simple nanoscale particles have very small tap density (less than 1.0 g cm^{-3}) and can easily fall off from the aluminum foil. Micro-sized $LiFePO_4$/C composites have high tap density (for example, tap density as high as 1.6 g cm^{-3} can be reached[18]) and are generally used in manufacturing real batteries for applications. These micro-nano hierarchical structured $LiFePO_4$/C composites showed a tap density of 1.4 g cm^{-3} and should be ready to be used as the cathode materials in real lithium ion batteries.

4. Conclusions

In summary, monoclinic phase $FePO_4 \cdot 2H_2O$ with micro-nano hierarchical structures are synthesized using a hydrothermal method and lithiated to $LiFePO_4$/C, which also has hierarchical structures, by a simple rheological phase method. These specially structured $LiFePO_4$/C materials show both excellent high-rate performance and high tap density as the cathode for lithium ion batteries. Discharge capacities of more than 120, 110, and 90 mAh g^{-1} at high rates of 5 C, 10 C and 20 C, respectively, and a tap density of 1.4 g cm^{-3} can be achieved at same time. These as-prepared materials are capable of large-scale applications, such as electric vehicles and plug-in hybrid electric vehicles.

Acknowledgements

The authors thank the Center for Electron Microscopy at Wuhan University for help in taking the TEM and high-resolution TEM images for the materials. This study was supported by the National Science Foundation of China (grant No. 20901062) and the Fundamental Research Funds for the Central Universities (grant No. 2082002).

References

1 J. M. Tarascon and M. Armand, *Nature*, 2001, **414**, 359–367.
2 M. Armand and J. M. Tarascon, *Nature*, 2008, **451**, 652–657.
3 P. G. Bruce, B. Scrosati and J. M. Tarascon, *Angew. Chem., Int. Ed.*, 2008, **47**, 2930–2946.

4 A. K. Padhi, K. S. Nanjundaswamy and J. B. Goodenough, *J. Electrochem. Soc.*, 1997, **144**, 1188–1194.
5 S.-Y. Chung, J. T. Bloking and Y.-M. Chiang, *Nat. Mater.*, 2002, **1**, 123–128.
6 S. Shi, L. Liu, C. Ouyang, D. S. Wang, Z. Wang, L. Chen and X. Huang, *Phys. Rev. B*, 2003, **68**, 1951081.
7 D. Wang, H. Li, S. Shi, X. Huang and L. Chen, *Electrochim. Acta*, 2005, **50**, 2955.
8 N. Ravet, J. B. Goodenough, S. Besner, *The 196th Meeting of the Electrochemical Society*, Honolulu, HI, 1999.
9 P. S. Herle, B. Ellis, N. Coombs and L. F. Nazar, *Nat. Mater.*, 2004, **3**, 147–152.
10 F. Croce, A. D. Epifanio, J. Hassoun, A. Deptula, T. Olczac and B. Scrosati, *Electrochem. Solid-State Lett.*, 2002, **5**, A47–A50.
11 Y. S. Hu, Y. G. Guo, R. Dominko, M. Gaberscek, J. Jamnik and J. Maier, *Adv. Mater.*, 2007, **19**, 1963–1966.
12 M. Gaberscek, R. Dominko and J. Jamnik, *Electrochem. Commun.*, 2007, **9**, 2778–2783.
13 Y. G. Wang, Y. R. Wang, E. Hosono, K. X. Wang and H. S. Zhou, *Angew. Chem., Int. Ed.*, 2008, **47**, 7461–7465.
14 C. Delacourt, P. Poizot, S. Levasseur and C. Masquelier, *Electrochem. Solid-State Lett.*, 2006, **9**, A352.
15 D. Choi and P. N. Kumta, *J. Power Sources*, 2007, **163**, 1064–1069.
16 Z. Chen and J. R. Dahn, *J. Electrochem. Soc.*, 2002, **149**, A1184–A1189.
17 R. Dominko, M. Bele, J.-M. Goupil, M. Gaberscek, D. Hanzel, I. Arcon and J. Jamnik, *Chem. Mater.*, 2007, **19**, 2960–2969.
18 H.-M. Xie, R. S. Wang, J. R. Ying, L. Y. Zhang, A. F. Jalbout, H. Y. Yu, G. L. Yang, X. M. Pan and Z. M. Su, *Adv. Mater.*, 2006, **18**, 2609–2613.
19 L. N. Wang, Z. G. Zhang and K. L. Zhang, *J. Power Sources*, 2007, **167**, 200–205.
20 M. Wang, Y. H. Xue, K. L. Zhang and Y. X. Zhang, *Electrochim. Acta*, 2011, **56**, 4294–4298.
21 X. M. Lou and Y. X. Zhang, *J. Mater. Chem.*, 2011, **21**, 4156–4160.
22 B. Liu, S. H. Yu, L. Li, F. Zhang, Q. Zhang, M. Yoshimura and P. Shen, *J. Phys. Chem. B*, 2004, **108**, 2788.
23 T. He, D. Chen, X. Jiao, Y. Xu and Y. Gu, *Langmuir*, 2004, **20**, 8404.
24 T. He, D. Chen and X. Jiao, *Chem. Mater.*, 2004, **16**, 737.
25 J. J. Chen and M. S. Whittingham, *Electrochem. Commun.*, 2006, **8**, 855.
26 J. S. Chen, Y. L. Cheah, Y. T. Chen, N. Japaprakash, S. Madhavi, Y. H. Yang and X. W. Lou, *J. Phys. Chem. C*, 2009, **113**, 20504.
27 X. W. Lou, D. Deng, J. Y. Lee and L. A. Archer, *Chem. Mater.*, 2008, **20**, 6562.
28 G. X. Wang, H. Liu, J. Liu, S. Z. Qiao, G. Q. Lu, P. Munro and H. J. Ahn, *Adv. Mater.*, 2010, **22**, 4944.
29 D. Rangappa, K. Sone, M. Ichihara, T. Kudo and I. Honma, *Chem. Commun.*, 2010, **46**, 7548.
30 K. Saravanan, M. V. Reddy, P. Balaya, H. Gong, B. V. R. Chowdari and J. J. Vittal, *J. Mater. Chem.*, 2009, **19**, 605.